frontiers in Earth Science

ORIGINAL RESEARCH
published: 09 April 2019
doi: 10.3389/feart.2019.00071

Stratigraphic Occurrences of Sub-Polar Planktic Foraminifera in Pleistocene Sediments on the Lomonosov Ridge, Arctic Ocean

Matt O'Regan[1,2], Helen K. Coxall[1,2], Thomas M. Cronin[3], Richard Gyllencreutz[1,2], Martin Jakobsson[1,2], Stefanie Kaboth[4,5], Ludvig Löwemark[5], Steffen Wiers[6] and Gabriel West[1,2]*

[1] Department of Geological Sciences, Stockholm University, Stockholm, Sweden, [2] Bolin Centre for Climate Research, Stockholm University, Stockholm, Sweden, [3] Florence Bascom Geoscience Center U.S. Geological Survey, Reston, VA, United States, [4] Institute of Earth Sciences, Heidelberg University, Heidelberg, Germany, [5] Department of Geosciences, National Taiwan University, Taipei, Taiwan, [6] Department of Earth Sciences, Natural Resources and Sustainable Development, Uppsala University, Uppsala, Sweden

OPEN ACCESS

Edited by:
Michaël Hermoso,
UMR7193 Institut des Sciences de la Terre Paris (ISTEP), France

Reviewed by:
Teodora Pados,
Aarhus University, Denmark
Michal Kucera,
University of Bremen, Germany
Chiara Consolaro,
Marine Biological Association, United Kingdom

***Correspondence:**
Matt O'Regan
matt.oregan@geo.su.se

Specialty section:
This article was submitted to Quaternary Science, Geomorphology and Paleoenvironment, a section of the journal Frontiers in Earth Science

Received: 29 November 2018
Accepted: 19 March 2019
Published: 09 April 2019

Citation:
O'Regan M, Coxall HK, Cronin TM, Gyllencreutz R, Jakobsson M, Kaboth S, Löwemark L, Wiers S and West G (2019) Stratigraphic Occurrences of Sub-Polar Planktic Foraminifera in Pleistocene Sediments on the Lomonosov Ridge, Arctic Ocean. Front. Earth Sci. 7:71. doi: 10.3389/feart.2019.00071

Turborotalita quinqueloba is a species of planktic foraminifera commonly found in the sub-polar North Atlantic along the pathway of Atlantic waters in the Nordic seas and sometimes even in the Arctic Ocean, although its occurrence there remains poorly understood. Existing data show that *T. quinqueloba* is scarce in Holocene sediments from the central Arctic but abundance levels increase in sediments from the last interglacial period [Marine isotope stage (MIS) 5, 71–120 ka] in cores off the northern coast of Greenland and the southern Mendeleev Ridge. *Turborotalita* also occurs in earlier Pleistocene interglacials in these regions, with a unique and widespread occurrence of the less known *Turborotalita egelida* morphotype, proposed as a biostratigraphic marker for MIS 11 (474–374 ka). Here we present results from six new sediment cores, extending from the central to western Lomonosov Ridge, that show a consistent Pleistocene stratigraphy over 575 km. Preliminary semi-quantitative assessments of planktic foraminifer abundance and assemblage composition in two of these records (LOMROG12-7PC and AO16-5PC) reveal two distinct stratigraphic horizons containing *Turborotalita* in MIS 5. Earlier occurrences in Pleistocene interglacials are recognized, but contain significantly fewer specimens and do not appear to be stratigraphically coeval in the studied sequences. In all instances, the *Turborotalita* specimens resemble the typical *T. quinqueloba* morphotype but are smaller (63–125 μm), smooth-walled and lack the final thickened calcite layer common to adults of the species. These results extend the geographical range for *T. quinqueloba* in MIS 5 sediments of the Arctic Ocean and provide compelling evidence for recurrent invasions during Pleistocene interglacials.

Keywords: Arctic Ocean, Lomonosov Ridge, Pleistocene, chronology, lithostratigraphy, planktonic foraminifera, *Turborotalita quinqueloba*, biostratigraphy

INTRODUCTION

The diversity of planktic foraminifera in polar oceans is lower than in mid- and low latitude settings, with assemblages generally dominated by *Neogloboquadrina pachyderma*, followed by *Globigerenita uvula,* with occasional contributions of *Turborotalita quinqueloba* and *Globigerina bulloides* (Eynaud, 2011; Husum and Hald, 2012; Schiebel et al., 2017). In the Arctic Ocean and its marginal seas (**Figure 1**), *N. pachyderm* dominates planktic assemblages in both plankton tows and surface sediment samples (Carstens and Wefer, 1992; Stein, 2008; **Figure 2**). *T. quinqueloba* has been recovered in plankton tows from the Nansen Basin (Volkmann, 2000b) and Laptev Sea (Carstens and Wefer, 1992) but is scarcely recognized in Holocene sediments from the inner Arctic Ocean (Nørgaard-Pedersen et al., 2007; Stein, 2008; Adler et al., 2009; Eynaud et al., 2009). It is commonly described as a sub-polar species, abundant in the North Atlantic, in areas of the Nordic Seas influenced by inflowing Atlantic waters (Kucera et al., 2005a; Pados and Spielhagen, 2014), and in proximity to the marginal ice zone (Risebrobakken and Berben, 2018; **Figure 2**).

Increased abundances of *T. quinqueloba* are found in some inner Arctic sediment records during older Pleistocene interglacials (Herman, 1974; Poore et al., 1993, 1994; Jakobsson et al., 2001; Backman et al., 2004; Adler et al., 2009; Hanslik, 2011). In sediment cores recovered close to the Greenland margin (GreenICE core 11, LOMROG07-4PC), *T. quinqueloba* is particularly prolific in MIS 5.1 (∼82 ka), and 5.5 (∼123 ka) (Nørgaard-Pedersen et al., 2007; Hanslik, 2011; **Figure 1**). It appears earlier than MIS 5 in records from the westernmost Lomonosov Ridge off Greenland (LOMROG07-4PC) (Hanslik et al., 2013; Löwemark et al., 2016) and in many records from the western Arctic Ocean (Herman, 1974; Poore et al., 1993), but the timing of these events remains ambiguous.

A less well-known morphotype of *Turborotalita*, *Turborotalita egelida* (Cifelli and Smith), has also been identified in pre-MIS 5 sediments from the Northwind Ridge, Mendeleev Ridge, and the Lomonosov Ridge off Greenland (Cronin et al., 2013, 2014; Polyak et al., 2013; **Figure 1**). Its apparently unique stratigraphic occurrence has been proposed as a marker for MIS 11 (474–374 ka) (Cronin et al., 2013, 2014; Polyak et al., 2013). This not only suggests rather anomalous paleoceanographic conditions in the western and central Arctic Ocean during MIS 11, but potentially provides an important biostratigraphic event for correlation and dating of Arctic sediments (Polyak et al., 2013; Cronin et al., 2014). This is particularly important, as many of the more common Quaternary marine dating and correlation methods have unique problems in the Arctic (Backman et al., 2004; Alexanderson et al., 2014). These include the sporadic occurrence and limited diversity in many microfossil assemblages, the inability to generate a continuous and interpretable oxygen isotope stratigraphy from these assemblages, and the complex sequence of high frequency geomagnetic polarity reversals seen in many Arctic records (Clark, 1970; Spielhagen et al., 2004; O'Regan et al., 2008a; Xuan and Channell, 2010; Xuan et al., 2012) that are difficult to reconcile with the global geomagnetic polarity time scale or excursion records in the Quaternary (O'Regan et al., 2008a).

Despite difficulties in dating Arctic sediments, it is widely recognized that downcore lithologic variability can be correlated across large spatial distances (Clark et al., 1980; Sellén et al., 2010). For example, lithologic correlations between widely spaced cores exist for the Northwind Ridge (Phillips and Grantz, 2001), East Siberian and Chukchi margins (Schreck et al., 2018), Mendeleev and Alpha Ridges (Sellén et al., 2010), and eastern Lomonosov Ridge off Siberia (Stein et al., 2010). On the central Lomonosov Ridge, multiple records have been correlated to the longer Quaternary sequence recovered during *ACEX* (O'Regan et al., 2008a; Löwemark et al., 2012, 2014; **Figure 3**). Despite well-developed regional stratigraphies establishing the chronology of these sequences and the ability to correlate between regions, has proven very difficult.

On the central Lomonosov Ridge (**Figure 3**) there is a generally accepted late Quaternary (MIS 7 – present, 243–0 ka) chronology (Jakobsson et al., 2001; Spielhagen et al., 2004; O'Regan, 2011). It is anchored in the first appearance of the calcareous nannofossil *Emiliana huxleyi* in AO96-12PC (Jakobsson et al., 2000, 2001; **Figures 1**, **3**). *E. huxleyi* evolved in sub-polar seas during MIS 8 (243–300 ka) (Thierstein et al., 1977), and its first occurrence in the Arctic is used to identify the last interglacial period (LIG) (MIS 5, 71–130 ka) (Backman et al., 2009). The acceptance of this age model, and the proposed first occurrence of *E. huxleyi* in the Arctic during MIS 5, is underpinned by subsequent constraints from optically stimulated luminescence dating of quartz grains from a nearby record (AO96-24SEL) (**Figure 3**; Jakobsson et al., 2003). The Quaternary age model for the *ACEX* record extended this chronological framework by combining long-term (Neogene) estimates of sedimentation rates derived from the decay of beryllium isotopes ($^{10}Be/^{9}Be$) (Frank et al., 2008) with cyclostratigraphic analyses of lithologic changes in the upper 20 m of the borehole (Backman et al., 2008; O'Regan et al., 2008a). The ambiguity of the paleomagnetic record, lack of an isotope stratigraphy, or biostratigraphic markers pre-dating MIS 5 leave notable uncertainty in this proposed Pleistocene chronology. The very limited occurrences of calcareous microfossils below MIS 5 in the *ACEX* record (and many surrounding sediment cores) have severely hampered our ability to correlate this stratigraphic sequence to more microfossil-rich sequences recovered from the western Arctic Ocean and in areas north of Greenland (Marzen et al., 2016).

This study is based on preliminary investigations into the downcore abundances of calcareous plantkic and benthic foraminifera undertaken on a series of sediment cores from the portion of the Lomonosov Ridge located north of Greenland (**Figure 3**). It is motivated by the observation that sediments recovered closer to the Greenland margin appear to have better preserved and more persistent downcore occurrences of calcareous foraminifera compared to those recovered in the region of *ACEX* (Cronin et al., 2008; Hanslik, 2011; Marzen et al., 2016). Critically, an initial screening of one of these

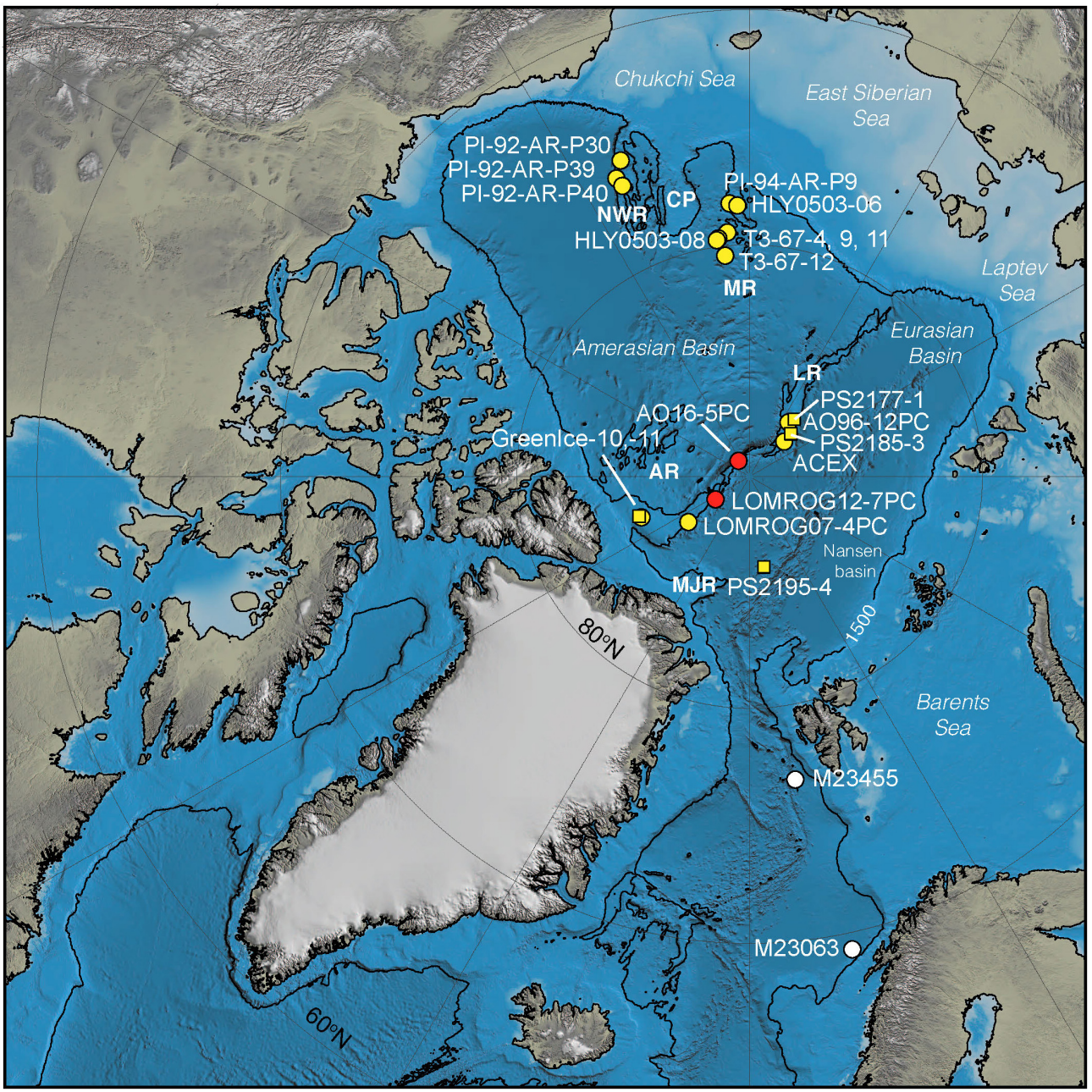

FIGURE 1 | Map of the Arctic Ocean illustrating sites where *Turborotalita* species have been described in Arctic Pleistocene sediments (yellow circles) and the new records presented in this manuscript (red circles). Yellow squares are box cores where abundances of *Turborotalita quinqueloba* were described in surface sediments by Nørgaard-Pedersen et al. (2007). References for published records are: P1-92- cores (Cronin et al., 2014), T3- cores (Herman, 1974). HYL0503-08 (Adler et al., 2009), HYL0503-06 (Cronin et al., 2013), ACEX (Eynaud et al., 2009), 96/12-PC (Jakobsson et al., 2001), LOMROG07-4PC (Hanslik, 2011), and Greenlce (Nørgaard-Pedersen et al., 2007). SEM images of representative species of *T. quinqueloba* from MIS 5 and MIS 11 were acquired from two sites in the Norwegian-Greenland Seas (M23455, M23063) (white circles) and are shown in **Figure 7**. AR, Alpha Ridge; LR, Lomonosov Ridge; MR, Mendeleev Ridge; MJR, morris jesup rise; NWR, Northwind Ridge.

records (LOMROG12-7PC) unexpectedly revealed *Turborotalita* specimens in Pleistocene sediments pre-dating the LIG. This warrants a closer look into the stratigraphic occurrences, abundances, and the taxonomic relationship of these specimens to morphotypes of *T. quinqueloba* and *T. egelida*.

Here we present lithostratigraphic results from six new sediment cores from the Lomonosov Ridge that show a consistent downhole stratigraphy that can be traced over 575 km from the *ACEX* borehole toward the northern Greenland margin (**Figure 1**). Semi-quantitative foraminifer abundance data is

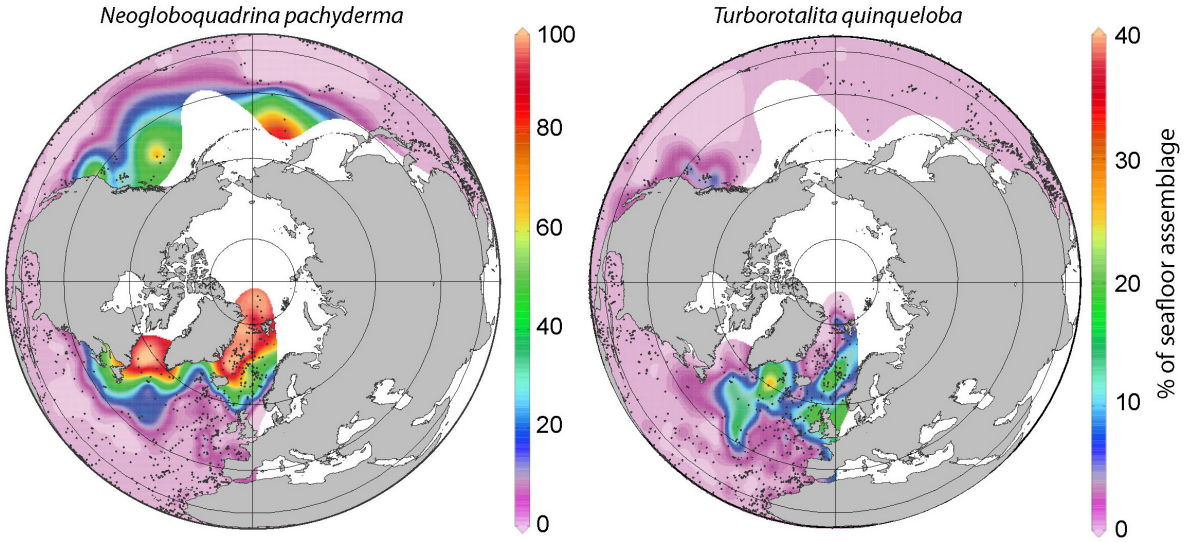

FIGURE 2 | Distribution of *Neogloboquadrina pachyderma* and *T. quinqueloba* in high northern latitude surface sediments. Gridded distributions produced with Ocean Data View (http://odv.awi.de) (Schlitzer, 2018) using the database from Kucera et al. (2005a) and published in Kucera et al. (2005b).

presented from two of these records (LOMROG12-7PC, AO16-5PC). Two distinct occurrences of the planktic foraminifer genus *Turborotalita* are found in these cores. Based on the chronology for the Quaternary section of ACEX, the occurrences are in MIS 5.1 and 5.5. An older occurrence of *Turborotalita* is also identified in both of these cores but it does not appear to be stratigraphically coeval. The morphology of specimens from all horizons resemble *T. quinqueloba* from the Nordic seas and not the *T. egelida* proposed as a biostratigraphic event marker for MIS 11.

MATERIALS AND METHODS

New sediment cores used in this study were collected during two icebreaker expeditions to the Arctic involving the Swedish icebreaker IB *Oden*. These were the joint Danish-Swedish Lomonosov Ridge off Greenland expedition in 2012 (LOMROG12) and the Canadian-Swedish Arctic Ocean 2016 (AO16) expedition with icebreakers IB *Oden* and the Canadian *Louis S. St-Laurent* (**Figure 3** and **Table 1**). During LOMROG12, piston cores (PC) were collected in transparent polycarbonate liners with an outer diameter (OD) of 88 mm and an inner diameter (ID) of 80 mm. During AO16, a larger diameter piston coring system was used, where cores were collected in white PVC liners with OD/ID of 110/100 mm. The piston corer was usually rigged to recover 9 m of sediment, although full penetration and/or 100% recovery was never achieved. A shorter 0.75–1.5 m long "*trigger weight core*" (TWC) was deployed along with each piston core. This shorter coring tool advances ahead of the piston core, and when it reaches the seabed, a mechanical trigger is released, allowing the piston core to free-fall 2–3 m before hitting the seabed. Due to the slower penetration of the TWC, they often recover a less disturbed seawater-sediment interface.

Sediment cores from LOMROG12 (LOMROG12-3PC/TWC, -6PC/TWC, -7PC, -12PC) were split and described on board. They were stored in a refrigerated container before being transferred to the cold storage room at Stockholm University at the end of the expedition. Sediment physical properties (Bulk Density, Magnetic Susceptibility, and P-wave velocity) were measured 2–3 months post-cruise on the archived split sections of the piston cores with a Geotek multi-sensor core logger (MSCL). Cores from AO16 (AO16-5PC and -12PC) were measured on board with a MSCL prior to splitting.

Archived sections from all the cores were scanned using an Itrax XRF core scanner at the Department of Geological Sciences, Stockholm University. XRF scanning was performed using a Mo tube set at 55 kV and 50 mA with a step size of 2 mm and an exposure time of 25 s. Elemental data were normalized by Ti, a conservative element commonly found in weathering resistant minerals, which consistently produces analytically reliable counting statistics on the Itrax XRF core scanner. After manually cleaning and removing poor quality measurements, the data were re-sampled at a resolution of 2 mm and smoothed with a 5-point running average.

Sediment grain size (2 μm–2 mm) was measured on cores LOMROG12-6PC at 1 cm downcore resolution, and on LOMROG12-7PC and -12PC at a 2 cm downcore resolution using a Malvern Mastersizer 3000 laser diffraction particle size analyzer. Wet samples were immersed in a dispersing agent (<10% sodium hexametaphosphate solution) and placed in an ultrasonic bath to facilitate particle disaggregation before analyses. The Malvern instrument was run with 30 s measurement duration at 5–12% obscuration level. The grain size data was analyzed based on Mie scattering in 71 size classes from 0.055 μm (very fine clay) to 3500 μm (coarse sand). Particle size

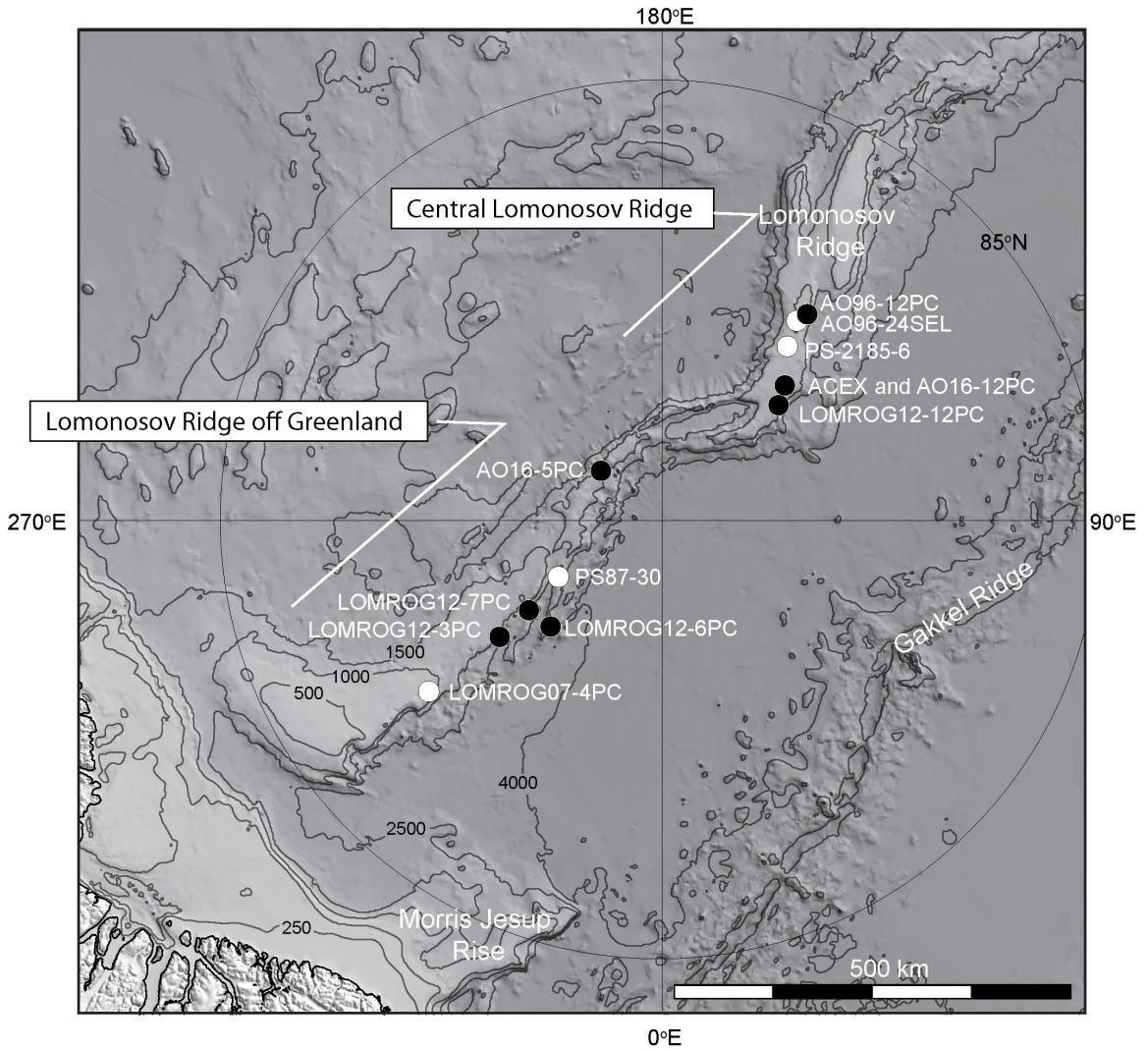

FIGURE 3 | Bathymetric map of the central and western Lomonosov Ridge showing locations of sediment cores discussed in the text. Black circles are cores for which a coherent downhole lithostratigraphy is shown in **Figure 5**, or in the case of AO96-12PC has been illustrated in previous work (O'Regan et al., 2008a,b) and is shown in **Figure 10**. White circles are locations of other cores discussed in the text. Core AO16-12PC was collected at the location on the Lomonosov Ridge drilled in 2004 during ACEX. At the resolution of this map they are both represented by the same black circle.

TABLE 1 | Core locations, water depths, and length.

Expedition	Core	Latitude (°N)	Longitude (°E)	Water depth (m)	Length (m)
LOMROG12	3PC	87.7247	−54.4253	1607	3.73
LOMROG12	6PC	88.2511	−46.3972	2923	6.59
	06TWC				0.55
LOMROG12	7PC	88.1976	−55.6845	2952	6.83
LOMROG12	12PC	88.1085	134.6451	1366	7.27
	12TWC				0.49
AO16	5PC	89.0780	−130.5470	1253	6.16
AO16	12PC	87.8577	136.9875	1269	5.19

classes were taken from European Standard EN ISO 14688-1:2018 (2018). Clay is defined as the 0–2 μm fraction, fine silt 2–6.3 μm, medium silt 6.3–20 μm, and coarse silt 20–63 μm.

Radiocarbon dates were acquired from 15 samples containing 400–700 specimens of *N. pachyderma* from LOMROG12-6PC/TWC, -7PC, and -12PC/TWC. They

TABLE 2 | Radiocarbon dating results from LOMROG12 cores.

Core	Sec.	Interval (cm)	Composite depth (mbsf)	Lab. code	^{14}C age (a BP)	1σ error	Med. cal. age (cal. a BP)	Age range (cal. a BP)
6TWC	1	1	0.01	LuS 10958	5120	105	4980	4410–5540
6PC	1	2.5	0.085	Beta 372217	6860	30	6950	6490–7380
6TWC	1	16	0.160	Beta 372218	27070	150	30530	29850–30980
6PC	1	18.5	0.245	Beta 372219	>43500			
6TWC	1	38	0.380	Beta 372220	>43500			
6PC	1	34	0.400	Beta 372221	>43500			
7PC	1	10.5	0.105	Beta 457945	5440	30	5360	4850–5830
7PC	1	25.5	0.255	Beta 457946	35070	300	38780	37900–39690
7PC	1	40.5	0.415	Beta 457948	39380	460	42590	41910–43280
7PC	1	85.5	0.855	Beta 457947	>43500			
12TWC	1	1	0.010	LuS 10952	3010	60	2300	1790–2780
12TWC	1	13	0.130	Beta 457835	11480	30	12560	11970–13020
12PC	1	13.5	0.205	Beta 457832	21930	80	24450	24920–25900
12TWC	1	21	0.210	Beta 457834	35420	290	39140	38440–39930
12TWC	1	33	0.330	Beta 457833	40500	530	43410	42560–44410

were measured at the Lund University Radiocarbon Dating Laboratory, Sweden (LuS), or Beta Analytic (Beta) (**Table 2**). Radiocarbon dates were converted to calendar ages using the Marine13 calibration curve (Reimer et al., 2013) and the CALIB 7.1 online radiocarbon calibration program (Stuiver et al., 2018). A ΔR of 400 $\pm$ 200 years was applied to all samples although it is acknowledged that this may underestimate the true marine radiocarbon reservoir age at the different coring sites, especially in glacial and deglacial sediments (Hanslik et al., 2010). All calibrated results are rounded to 10 years and reported at the 95.4% (2-sigma) confidence limit. Visual comparison and correlation of XRF scanning results were used to establish a composite depth scale for LOMROG12-6PC/TWC and for LOMROG12-12PC/TWC. In the composite depth scales (reported in meters composite depth – mcd), 6.5 cm were added to measured core depths in LOMROG12-6PC, and 5 cm to measured core depths in LOMROG12-12PC. No composite depth scale was generated for LOMROG12-7PC, as the TWC on this deployment came up empty.

Samples for foraminifera analyses were taken from LOMROG12-7PC and AO16-5PC using 2 cm wide, 10 cm^3 plastic scoops. Extracted samples were freeze-dried, weighed, wet sieved over a 63 μm sieve and dried in an oven at 50°C for 2–3 h. Downcore sampling was generally conducted at a resolution of 8–10 cm but varied depending on core lithology. In some instances, the sampling resolution was increased in intervals where *Turborotalita* was identified. Semi-quantitative estimates of calcareous planktic and benthic and agglutinated foraminifera were made on the >125 μm fraction using a scale where: Abundant ≥50% of sample, Common >100 specimens, Few = 50–100 specimens, Rare <50 specimens, and Barren = 0 specimens. Absolute numbers of foraminifera have not been counted, and so no quantitative information on foraminifera/g of dry sediment is available. During this initial work, a few specimens of *Turborotalita* specimens were identified which motivated us to look at the smaller size fractions (63–125 μm) to establish its stratigraphic distribution. When *Turborotalita* were found in the 63–125 μm fraction, notes were made on the assemblage composition and its relative abundance in the smaller size fraction.

Scanning electron microscope images of representative specimens identified as *Turborotalita* in LOMROG12-7PC were obtained using a Philips XL-30- ESEM-FEG environmental scanning electron microscope housed at Stockholm University. Specimens were gold coated and imaged under high vacuum (10 kV) using a working distance of 11.2 mm. This was done to document test sizes and morphology to aid taxonomic assignment. Images were compared to the *Turborotalita* type material from the Cushman Collection held at the United States National Museum (USNM)[1] and Pleistocene core samples from the Norwegian Greenland Sea.

RESULTS

Lithologic Correlation and Stratigraphy

Grain size provides a simple stratigraphic correlation tool for sediments from the central Arctic Ocean (Spielhagen et al., 2004; O'Regan et al., 2010). High-resolution measurements of sediment bulk density (O'Regan et al., 2008b; Sellén et al., 2010; Löwemark et al., 2014) and manganese content (Jakobsson et al., 2000; Löwemark et al., 2014) have also been extensively used to correlate sediment cores from the Lomonosov Ridge. Manganese, although susceptible to post-depositional remobilization, tends to be enriched in interglacial and interstadial sediments (Jakobsson et al., 2000; Löwemark et al., 2014), while grain size is suggested as the primary source of downcore variation in sediment bulk density (O'Regan et al., 2008a, 2014).

[1] https://collections.nmnh.si.edu/search/paleo/

In the three grain-size records presented here (LOMROG12-6PC, -7PC, and -12PC), there is a high degree of correlation between bulk density and the coarse silt and sand content (cross-correlation coefficients for the mean removed and resampled data series between 0.823 and 0.898) and inverse correlation to the clay and fine silt content (−0.866 to −0.912) (**Figure 4** and **Table 3**). Adding the fine silt fraction to the clay and the coarse silt fraction to the sand increases the cross-correlation coefficients in all three cores (**Table 3**). The same downcore variability seen in the bulk density and grain size data is also captured by the Zr/Ti ratio, commonly used as a proxy for grain size in marine and lacustrine sediments (Rothwell and Croudace, 2015; Chawchai et al., 2016).

Despite large variations in sedimentation rate, downcore variations in bulk density and Zr/Ti can be correlated across a large stretch of the Lomonosov Ridge (**Figure 5**). Two relatively thick coarse-grained units (diamicts) are present in all of these cores (D_A, D_B in **Figure 5**). These diamicts are usually found in the upper few meters from the seafloor. Regionally, they contain intervals of light to dark gray sediments and variably colored coarse- and fine-grained laminae. Based on the current chronology from *ACEX* (O'Regan et al., 2008a; O'Regan, 2011), AO96-12PC (Jakobsson et al., 2001), and PS-2185-6 (Spielhagen et al., 2004; **Figure 3**), the lowermost diamict was deposited during MIS 6 (191–130 ka), and the uppermost one during MIS 3/4 (between ∼50 and ∼71 ka). Across the Lomonosov Ridge, radiocarbon dating has shown that deposition of the most recent diamict certainly ended prior to 40–50 ka (Nørgaard-Pedersen et al., 1998). This is consistent with the radiocarbon results presented for LOMROG12-6PC, -7PC, and -12PC/TWC (**Figure 4** and **Table 2**).

Below the lowermost diamict (D_B), there is a characteristic sequence of 3 rather rounded, coarser-grained, tan colored units (α, β, γ) (**Figure 5**). These features are present, but less well expressed, in the more compressed (lower-sedimentation rate) records of LOMROG12-3PC and AO16-05PC. The base of this sequence coincides with a very fine-grained unit of peach colored clay that can be seen visually or recognized by its low bulk density (red line labeled PL in **Figure 5**). Below this level, correlations between the cores become more tenuous, as many records exhibit far less pronounced variations in grain size or the respective proxies (bulk density and Zr/Ti). The general correlation between these cores based on the grain size proxies of bulk density and Zr/Ti are further supported by K/Ti and Mn/Ti (**Supplementary Figures S1**, **S2**).

Planktic Foraminifera

LOMROG12-7PC: Observations on the >63 μm fractions in LOMROG12-7PC revealed that planktic foraminifera are common to abundant down to 1.78 m subsurface, below which they become rare to common or absent (**Figure 6**). Benthic foraminifera are also relatively common in the upper 1.78 m and rare to absent below. Assemblages of planktic foraminifera are dominated by *N. pachyderma*, with are variety of morphotypes found, including large five-chambered, and small non-encrusted morphotypes described previously in the ACEX record by Eynaud et al. (2009).

There are three intervals in LOMROG12-7PC where *Turborotalita* is recorded: section 2, 7–9 cm to 17–19 cm (0.88–0.98 mcd); section 2, 81–83 cm to 91–93 cm (1.62–1.72 mcd); and section 3, 122–124 cm to 134–136 cm (3.54–3.66 mcd). In all cases the specimens referred to as *Turborotalita* are almost exclusively in the 63–125 μm fraction. Occasionally, 1–2 individuals are found in the >125 μm fraction. In the 63–125 μm fraction, *Turborotalita* represent a minor component (up to 20–40%) of assemblages, otherwise dominated by *N. pachyderma*, with a lower overall foraminifera abundance (rare to common) in the deeper stratigraphic levels compared to the two shallower occurrences (common to abundant).

AO16-5PC: Common to abundant planktic foraminifera occur in the >63 μm size fraction down to a depth of 3.40 m in AO16-5PC. This level is stratigraphically lower than the common to abundant zones in LOMROG12-7PC (**Figure 6**). Increased abundances of benthic calcareous foraminifera co-occur with the planktics through this interval. Expectedly, foraminifera become rare or absent from the two diamict units. Planktic assemblages are again dominated by morphotypes of *N. pachyderma*.

Similar to LOMROG12-7PC, there are three intervals in AO16-5PC where *Turborotalita* species are identified: section 1, 94–104 cm (0.94–1.04 m); section 1, 142 cm to section 2, 2 (1.42–1.54 m); and section 3, 130–136 cm (2.82–2.88 m). Again, specimens of *Turborotalita* are almost exclusively in the 63–125 μm fraction with only a few examples found in >125 μm fraction. Relative abundances of *Turborotalita* species are highest in the interval 1.42–1.54 m, where they are well preserved and account for 30–50% of the foraminifera in the 63–125 μm fraction. Relative abundances are less in the overlying interval (0.94–1.04 m) where they account for approximately 5–30% of individuals in the 63–125 μm fraction and vary between samples. The lowermost interval (2.82–2.88 m) contains less abundant foraminifera. The planktic assemblage is dominated by morphotypes of *N. pachyderma* found in the >125 μm fraction. Substantial amounts of pyrite were noted in these samples and extremely rare occurrences (<10 individuals) of *Turborotalita* were found in the 63–125 μm fraction.

Morphological Observations

The *Turborotalita* species found in LOMROG12-7PC and AO16-5PC show morphological characteristics indicative of the species *T. quinqueloba* (Natland). SEM micrographs of representative morphologies from several samples from LOMROG12-PC07 are presented (**Figures 7**, **8**, all specimens to scale). Taxonomically important features include enrolled coiling and an ampulate final chamber that extends into the umbilicus. Close-up images of the wall textures reveal spine bases confirming the presence of spines and thus affinity to family Globigerinidae (**Figure 7**, image 8; **Figure 8**, image 10). An important observation is that the central Arctic forms are typically small (mostly <125 μm), have smooth wall surfaces between spine bases and appear translucent under the light microscope. This contrasts with *T. quinqueloba* from low latitude and subpolar regions,

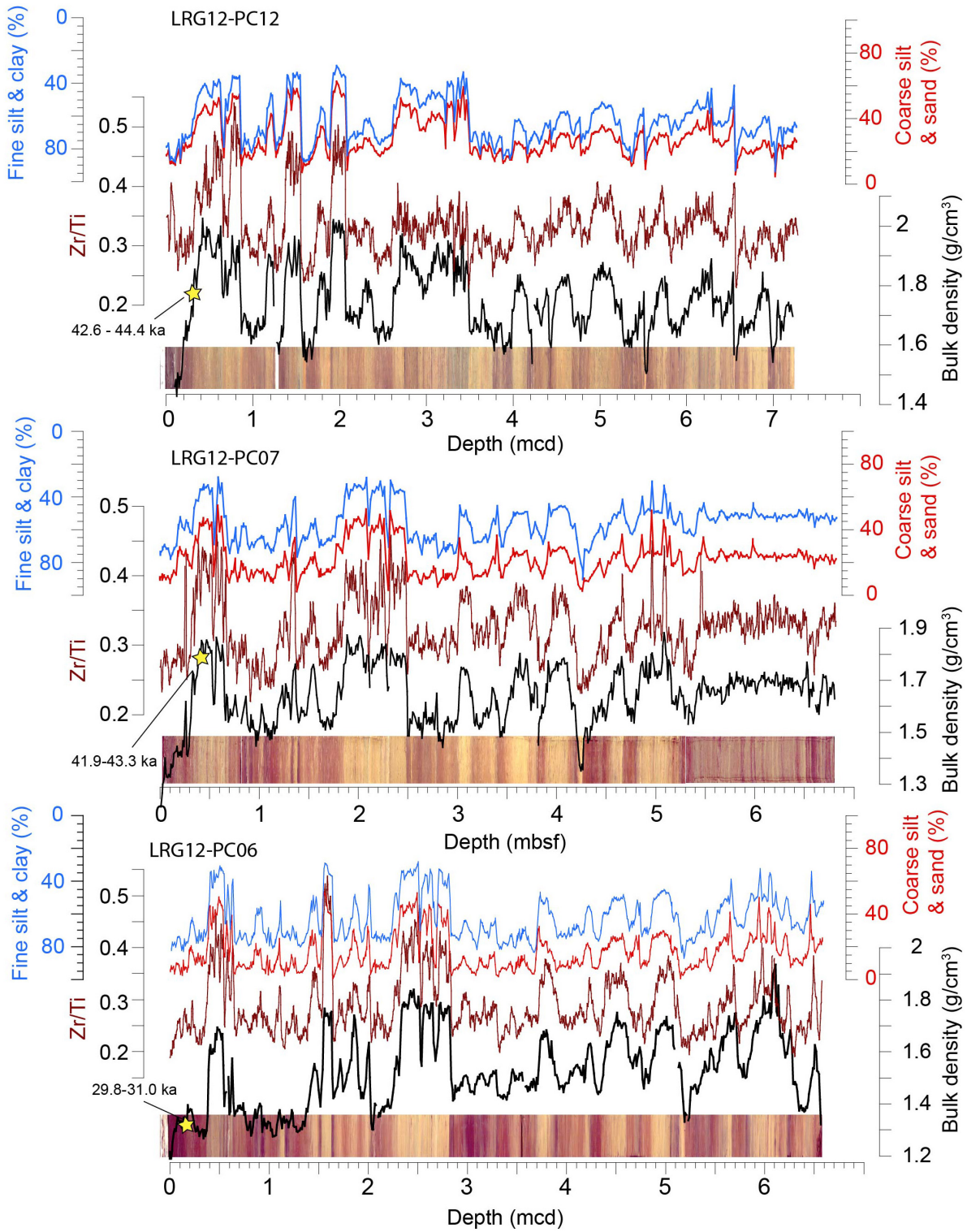

FIGURE 4 | Downhole core records of bulk density, Zr/Ti, and grain size for three records from the Lomonosov Ridge. Grain size data is presented as the % volume of different size fractions. A high degree of correlation exists between all these parameters – supporting the use of bulk density or Zr/Ti as proxies for bulk grain size. The 2-sigma ranges of the oldest finite radiocarbon dates for each core are shown (yellow star). A complete list of radiocarbon dates for each core is given in **Table 2**. Core depths are reported in either meters beneath the seafloor (mbsf) or meters composite depth (mcd).

TABLE 3 | Correlation coefficients between bulk density and grain size parameters.

Core	Clay (0–2 μm)	Silt (2–63 μm)	Sand (>63 μm)	Fine silt (2–6.3 μm)	Medium silt (6.3–20 μm)	Coarse silt (20–63 μm)	Fine silt + clay	Coarse silt + sand
LOMROG12-12PC	−0.795	−0.449	0.692	−0.771	−0.116	0.656	−0.866	0.835
LOMROG12-7PC	−0.840	0.099	0.656	−0.793	0.547	0.809	−0.882	0.823
LOMROG12-6PC	−0.891	0.045	0.829	−0.883	0.597	0.868	−0.912	0.898

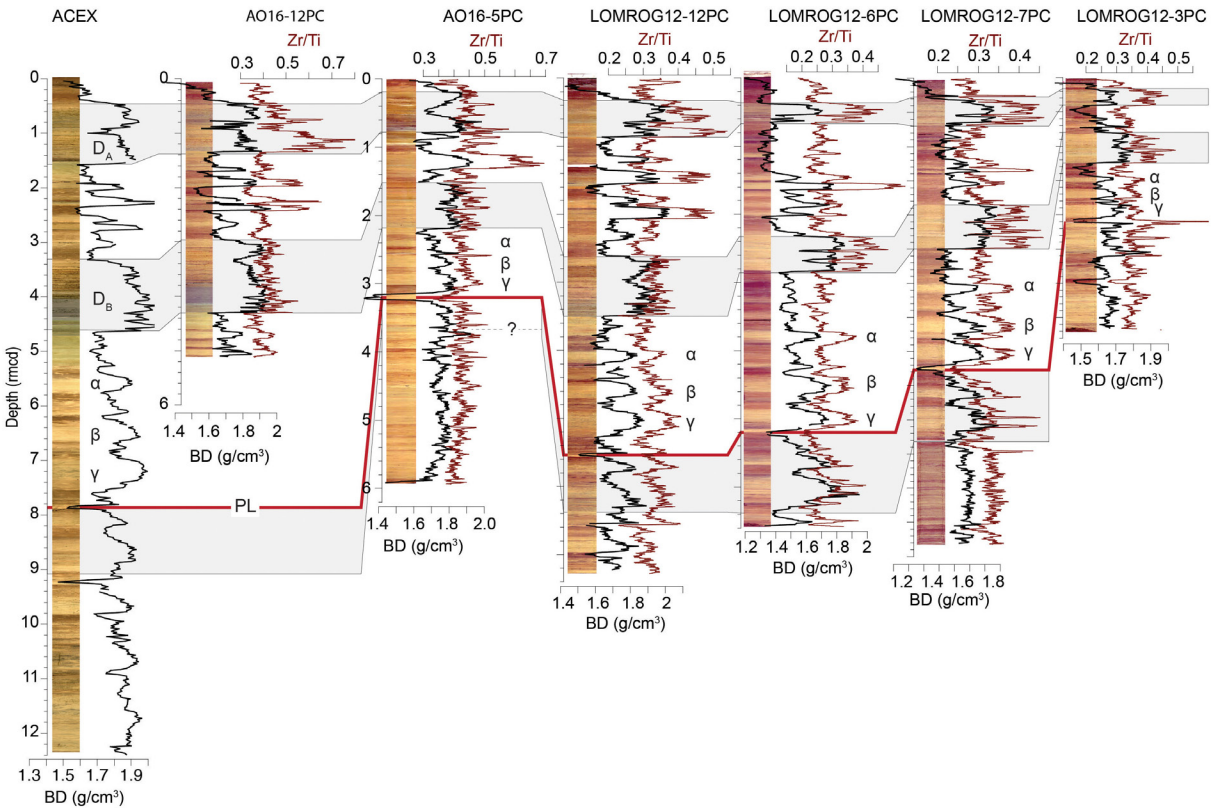

FIGURE 5 | Stratigraphic correlation of multiple records across ~575 km of the Lomonosov Ridge (see **Figure 3** for core locations). Correlations are shown using the bulk density and Zr/Ti proxies for grain size. They are further supported by downcore changes in sediment color (images) as well as K/Ti and Mn/Ti profiles (**Supplementary Information**). The bold red correlative line indicates the position of a distinct fine-grained (95–100% clay) peach colored layer (labeled PL). Greek symbols (α, β, γ) highlight a correlative sequence of grain size and color variations that are recognized above the fine-grained peach colored layer (PL). The two diamicts found near the top of all the cores are labeled D_B and D_A.

which include many individuals larger than 125 μm that exhibit a covering of gametogenic calcite (referred to as a "smooth calcite crust" by Olsson and Hemleben (2006) creating a thickened and heavily textured appearance (**Figure 7**, images 13–15). AO16-5PC counterparts fall into similar size categories and have similarly good preservation to those from LOMROG12-7PC (not shown).

The *Turborotalita* from LOMROG12-7PC and AO16-5PC are substantially smaller than the Arctic specimens referred to as *T. egelida,* which also have a more rounded final chamber and a more open umbilicus (Cronin et al., 2014; **Figures 9c,d**). Notable variability exists between individual test morphologies in LOMROG12-7PC, and we do find examples having more rounded final chambers (**Figure 7**, image 6). These specimens are closer to the examples of *T. egelida* reported on the Northwind Ridge (Cronin et al., 2014), which show affinities with Cifelli and Smith (1970) holotype described from the North Atlantic (originally *Globigerina egelida*; **Figure 9**). However, small specimens having a rounded final chamber are also part of the MIS 5 populations of *T. quinqueloba* described in a Fram Strait core (**Figure 7**, image 14), implying both these morphologies occurred in the Norwegian Greenland Sea populations.

DISCUSSION

Morphology and Taxonomy

The morphologies of *Turborotalita* specimens from all horizons fall within the recognized variability of living

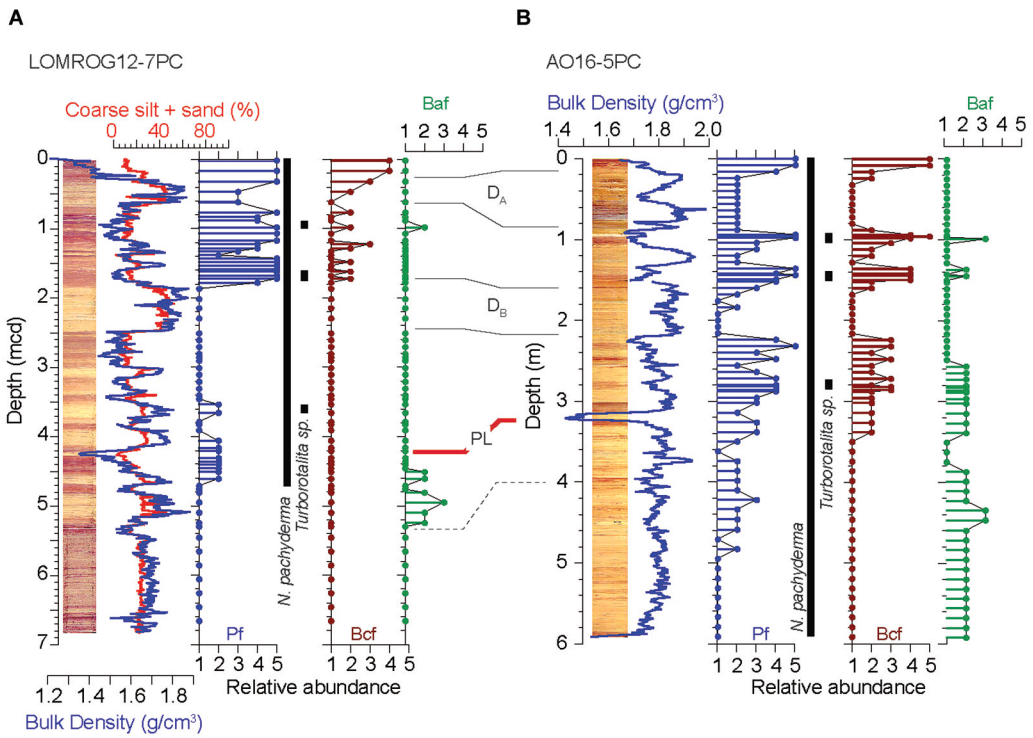

FIGURE 6 | Relative foraminifer abundance (>125 μm) and occurrences of *Turborotalita* (63–125 μm) in **(A)** LOMROG12-7PC and **(B)** AO16-5PC. Pf, planktic foraminifera; Bcf, benthic calcareous foraminifera; Baf, benthic agglutinated foraminifera. Numbers on the relative abundance scales correspond to: 5, abundant; 4, common; 3, few; 2, rare; 1, barren. The close association of bulk density and the coarse silt + sand content is shown for LOMROG12-7PC. Correlative stratigraphic features between these two cores are taken from **Figure 5**. Occurrence zone of *N. pachyderma* and *Turborotalita* spp. are shown alongside each core.

and fossil assemblages of *T. quinqueloba* from sub-polar seas. The main difference between these populations and the previously identified *T. egelida* zone in Arctic sediments (Cronin et al., 2014) appears to be in the low number of individuals, their small size and the tendency to possess an ampulate final chamber, which *T. egelida* lacks (**Figure 9**). Furthermore, where identified, *T. egelida* has been abundant in the larger (>150 um) size fractions and dominated the planktic foraminifera assemblages (Cronin et al., 2014).

The taxonomic and biological relationship between the reported *T. egelida* (evolute, large, and open umbilicus) and *T. quinqueloba* morphotypes remains unclear. Molecular studies have distinguished two cool water *Turborotalita* genotypes in the North Atlantic and Nordic Seas, including one species with bipolar distribution (Type IIa) and a distinct North Atlantic genotype (Type IIb) (Darling and Wade, 2008). It is unknown whether these genetic differences relate to observable morphological traits. It is possible that they are distinct, implying more than one species of *Turborotalita* that could have invaded the Arctic Ocean during warm periods of the Pleistocene. Resolving these taxonomic differences is particularly important for establishing the biostratigraphic significance of these events and for unraveling the environmental conditions that they represent.

At present *T. quinqueloba* shows maximum abundance in the Nordic seas along oceanic fronts, in particular the Arctic Front that separates Atlantic and Arctic Water masses (Johannessen et al., 1994; Pados and Spielhagen, 2014; Risebrobakken and Berben, 2018; **Figure 2**). The recorded incursions of *Turborotalita* in sediment cores from north of Greenland and on the Lomonosov Ridge were likely sourced from this stock. It is unlikely that their occurrence in the inner Arctic can be explained by advection of subpolar foraminifera from the Nordic Seas, and they likely represent a resident population as suggested by Kandiano and Bauch (2002) and Nørgaard-Pedersen et al. (2007). Their dominance in sediment cores from north of Greenland is certainly difficult to reconcile with the counter-clockwise circulation pathway for Atlantic water in the Arctic (Nørgaard-Pedersen et al., 2007). Other arguments against large-scale expatriation is that immature specimens would sink with their cytoplasm and the associated bacterial oxidation would result in dissolution of the thin test in the water column or at the seafloor (Michal Kucera, pers. comm.). Moreover, advection should transport a combination of growth stages while we observe *T. quinqueloba* of similarly small test sizes. It is more likely that these pulses indicate times of anomalously warm paleoceanographic conditions, perhaps with more open water and higher primary production sufficient to support endemic *T. quinqueloba* populations as first argued

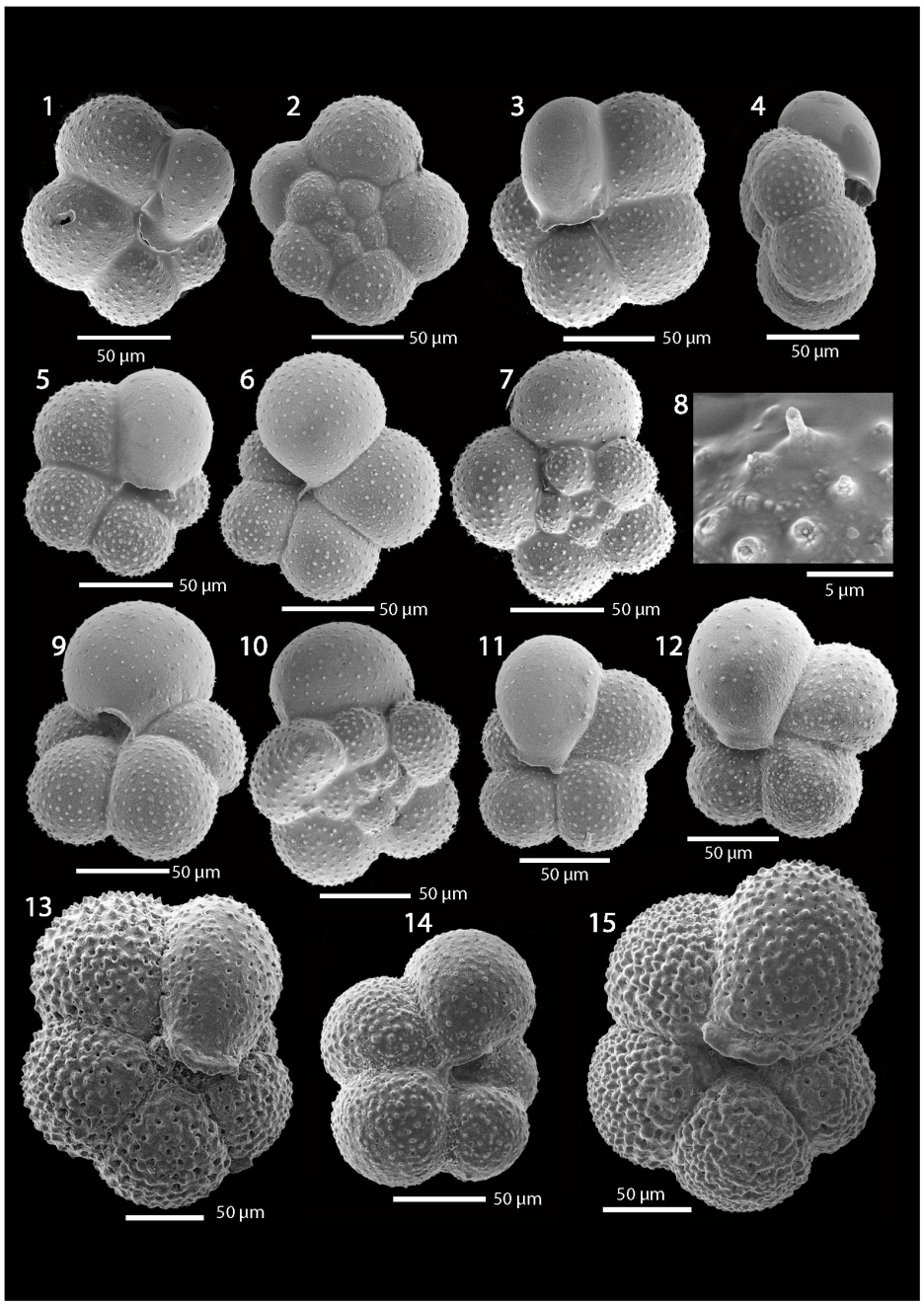

FIGURE 7 | SEM images of *Turborotalita* from Arctic and Sub-Arctic cores. Images 1–12; Well-preserved examples of *T. quinqueloba* from Sample LOMROG12 PC 0.7–2 cm and 7–9 cm (0.88 mbsf), probable MIS 5.1. Note these specimens lack an outer gametogenic crust typical of this species (compare to images 13 and 14) but often have the diagnostic ampulate final chamber. Images 1–2, 3–4, 6–8, and 9–10 are different views of the same specimen. The close-up test wall view (8) reveals a broken spine and spine bases diagnostic of the spinose wall texture of *T. quinqueloba.* Images 13 and 14 are *T. quinqueloba* from Core M23455, 309.25 cm subsurface, MIS 5, eastern Fram Strait (Van Nieuwenhove et al., 2011). Image 15 is *T. quinqueloba* from Core M23063, 733 cm subsurface, MIS 11, eastern Norwegian Greenland Sea (Bauch, 1997; Kandiano et al., 2012). Samples from M23063 and M23455 were provided by Antastasia Zhuravleva, GEOMAR Helmholtz Centre for Ocean Research, Kiel, Germany

by Nørgaard-Pedersen et al. (2007). However, the small size and absence of a typical gametogenic thickening suggests a different life history and even reproductive strategy. One possibility is that these were asexually reproducing forms. Asexual reproduction, common in benthic foraminifera, has been observed only once in planktic foraminifera in the species *Neogloboquadrina incompta* (Kimoto and Tsuchiya, 2006; Schiebel and Hemleben, 2017). It's entirely unknown whether *T. quinqueloba* does this but perhaps

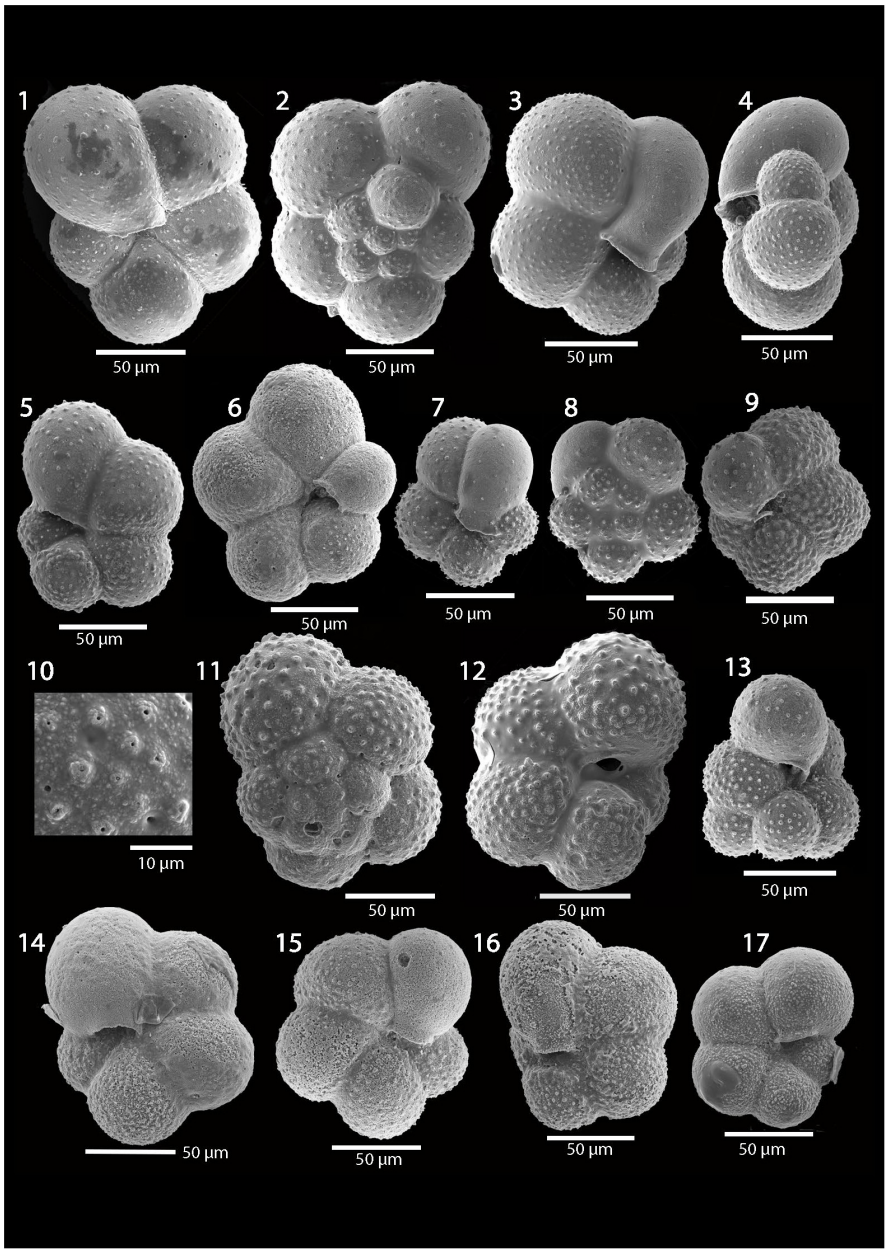

FIGURE 8 | SEM images of *Turborotalita* from the Lomonosov Ridge off Greenland in the Arctic Ocean. Images 1–13; Examples of *T. quinqueloba* from Sample LOMROG12-PC07, section 3, 114–116 cm (3.46 mbsf), probable MIS 9. Note these specimens lack the outer crust typical for this species but often have the diagnostic ampulate final chamber. Images 1–2, 3–4, 7–8, and 10–12 are different views of the same specimen. The close-up test wall view (10) reveals spine bases separated by smooth areas of test surface. Image 13 appears to be an aberrant form of *T. quinqueloba*. Images 14–16 are from LOMROG12-PC07, section 3, 114–116 cm (3.46 mbsf) proposed as MIS 9 age. Surfaces of the older specimens show traces of etching that can be likely attributed to partial dissolution.

asexual generation is an important strategy employed to survive the extremes and narrow limited growth periods of the central Arctic Ocean. The idea of resident central Arctic populations is also more consistent with observations of recurrent zones containing *T. quinqueloba* in numerous sediment cores from the western Arctic (Northwind and Mendeleev Ridges) (Herman, 1974; Poore et al., 1993; Adler et al., 2009) that are further removed from Atlantic water gateways into the Arctic.

Stratigraphic Occurrence

A novel aspect of this study is that the occurrences of *Turborotalita* are found within sediment cores that exhibit the same lithostratigraphy as at the ACEX site. This allows us to evaluate the coeval nature of their occurrences and provisionally date them through correlation to the cyclostratigraphic age model derived for ACEX (O'Regan et al., 2008a). Based on this correlation, coeval

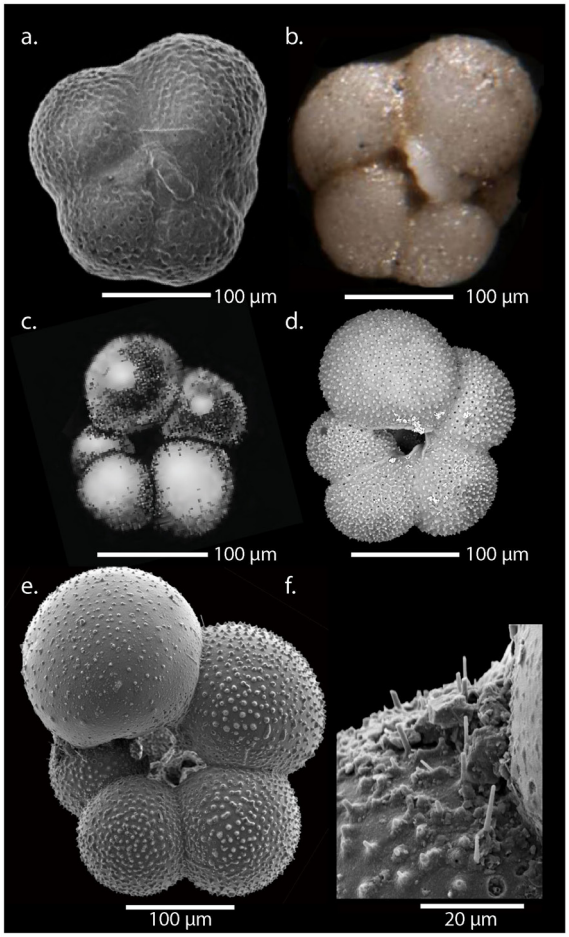

FIGURE 9 | (a) SEM and **(b)** light microscope images of the holotype of *T. quinqueloba* (Natland), USNM 3154044. **(c)** Type illustration of the holotype of *Globigerina egelida* Ciffelli and Smith (specimen lost from the USNM collection, Brian Huber, pers comm.). **(d)** SEM image of a paratype of *G. egelida* Ciffelli and Smith (USNM 179188). **(e)** A specimen identified as *Turborotalita egelida* from an interval interpreted as MIS 11 in core LOMROG07-4PC, 289–288 cm off Northern Greenland (Hanslik, 2011; Cronin et al., 2014). **(f)** Close up of image of **(e)** showing remnant spines indicative of the spinose family *Globigerinidae*.

appearances of *Turborotalita* species are found in LOMROG12-7PC and AO16-5PC during MIS 5 (very likely during substages 5.1 and 5.5), while earlier Pleistocene occurrences do not appear to be constrained to the same stratigraphic interval (AO16-5PC – MIS 11; LOMROG12-7PC – MIS9/10) (**Figure 10**).

The occurrences in MIS 5, very likely representing MIS 5.1 and 5.5, are consistent with occurrences of *T. quinqueloba* in AO96/12-1PC (Jakobsson et al., 2001; Backman et al., 2004), Green-Ice-11 (Nørgaard-Pedersen et al., 2007), LOMROG12-PC04 (Hanslik, 2011) and HLY0503-06 (Adler et al., 2009; **Figure 1**). Their generally small size matches observations made by Nørgaard-Pedersen et al. (2007) who found pulses of similarly small *T. quinqueloba* (63–125 µm) in GreenIce-11. Hanslik (2011) also found numerous intervals containing small *T. quinqueloba* in LOMROG07-4PC recovered closer to the Greenland margin on the Lomonosov Ridge than cores investigated in this study (**Figures 1**, **3**). In the initial age model for LOMROG07-4PC, these occurrences were in MIS 5, 7, and 9 (Hanslik, 2011; Löwemark et al., 2016). However, Hanslik (2011) recognized morphological differences between specimens in the lowermost interval, which were later interpreted as *T. egelida* and re-assigned to MIS 11 by Cronin et al. (2014).

The lower occurrence in LOMROG12-7PC is tentatively dated to MIS 9/10, while in AO16-5PC a few specimens are found in stratigraphically deeper sediments, assigned to MIS 11 (**Figure 10**). The MIS 9/10 occurrence in LOMROG12-7PC are stratigraphically coeval with elevated abundances of planktic foraminifera in the ACEX record, in which very few calcareous foraminifera were found in sediments older than MIS 1-3 (Cronin et al., 2008; Eynaud et al., 2009; **Figure 10**). Given the uncertainty in the cyclostratigraphic age model developed for *ACEX*, and relatively low inferred sedimentation rates in these new records, the older occurrences either align with (AO16-5PC) or are close to (LOMROG12-7PC) the assigned MIS 11 age for the *T. egelida* zone in western Arctic Ocean sediments (Cronin et al., 2014). However, dating of the *T. egelida* zone is also based on counting lithostratigraphic cycles interpreted to reflect successive glacial and interglacial cycles (Polyak et al., 2013). A problem with these cyclostratigraphic approaches lies in confidently resolving interglacial/glacial from interstadial/stadial deposits. Misinterpretations can easily introduce errors into the age models that exceed a single glacial cycle. Back to MIS 14, the cyclostratigraphic age model for ACEX is consistent with an earlier attempt to correlate Mn cycles in core 96/12-1PC on the Lomonosov Ridge to the Pleistocene MISs (Jakobsson et al., 2000; O'Regan et al., 2008a; Löwemark et al., 2014). However, no independent age control yet exists to verify these age models.

Recently, Hillaire-Marcel et al. (2017) published estimates of sedimentation rates at a nearby core on the Lomonosov Ridge (PS87/30, **Figure 3**) from extinction ages for ^{230}Th and ^{231}Pa. They use these results to argue for much lower late Quaternary sedimentation rates (4.3 mm /kyr) than reported for similar aged sediments from ACEX (2–3 cm/ka) (O'Regan et al., 2008a). However, further stratigraphic information is required to effectively evaluate these findings. Large regional variations in sedimentation rate can be expected and are seen in the lithostratigraphic correlations across this portion of the Lomonosov Ridge (**Figure 5**). For example, the depth to the base of the lower diamict (D_B) is ∼4.6 m at ACEX and only ∼1.2 m at LOMROG12-3PC. If the age assignment is correct (190 ka), this results in sedimentation rates between 2.42 cm/kyr (ACEX) and 0.63 cm/kyr (LOMROG12-3PC). While more progress on dating is needed to resolve boundaries of Pleistocene glacial/interglacial cycles in most Arctic sediment cores, the fact that *N. pachyderma* routinely exists prior to the earliest *Turborotalita* occurrences in both these cores certainly suggests the sediments are younger than late to middle Pleistocene in age. For example, genetic studies indicate that the modern *N. pachyderma* genotype found in northern polar regions evolved <1.5–1.8 Ma (Darling et al., 2007). Furthermore, it has long been argued that *N. pachyderma* adapted to coldwater conditions

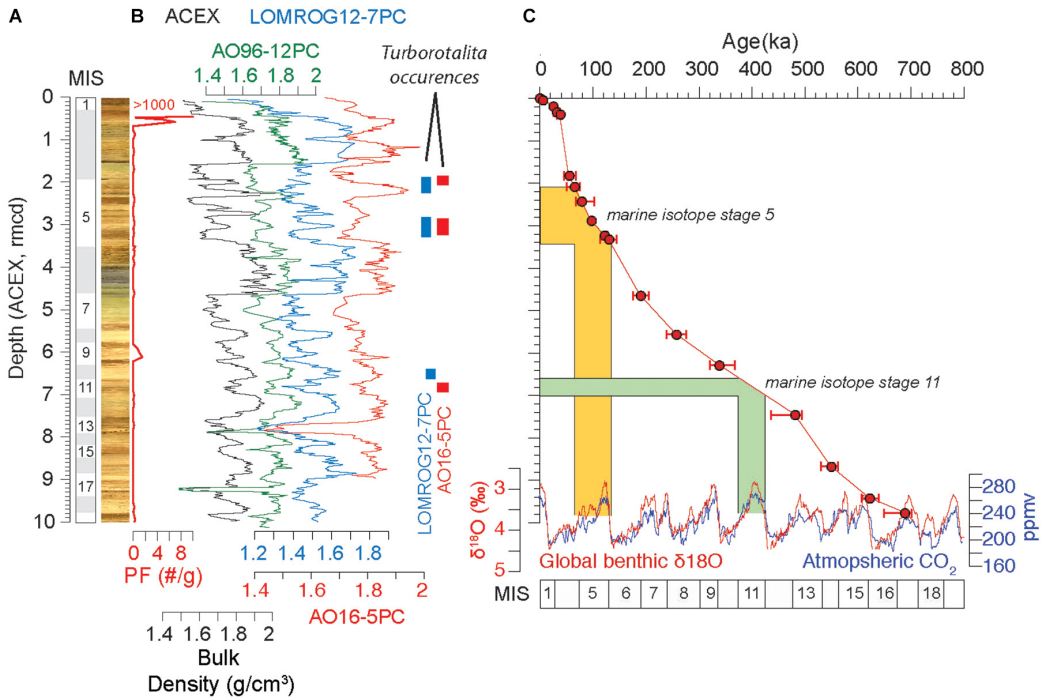

FIGURE 10 | (A) Summary stratigraphy from the upper 10 m of the ACEX borehole showing the composite core image and Planktic foraminiferal (Pf) abundance (individuals per dry gram of sediment) (Eynaud et al., 2009). **(B)** Bulk density data from ACEX (black), AO96-12PC (green), LOMROG12-7PC (blue), and AO16-5PC (red) are shown. They have been migrated onto the ACEX depth scale based on the stratigraphic correlation illustrated in **Figure 5**. The ACEX depth scale is the revised meters composite depth (rmcd) published for ACEX (O'Regan et al., 2008b). The location of the *Turborotalita* zones in LOMROG12-7PC and AO16-5PC are highlighted. **(C)** Age model for the upper 10 m of the ACEX borehole (O'Regan et al., 2008b) highlighting the interpreted depth intervals spanning MIS 5 and MIS 11. Global benthic oxygen isotope record and MIS boundaries are from Lisiecki and Raymo (2005). Atmospheric CO_2 concentrations are from a compilation of Antarctic ice core records (Lüthi et al., 2008). Two occurrences of *Turborotalita* in the LOMROG12-7PC and AO16-5PC appear to be stratigraphically coeval during MIS5, while the earlier occurrence in AO16-5PC appears older (MIS 11) compared to LOMROG12-7PC (MIS 9).

in the Norwegian-Greenland Seas between 1.0 and 1.1 Ma (Huber et al., 2000b).

Based on the size and morphological characteristics, specimens from MIS 5 and older occurrences all appear more similar to *T. quinqueloba* from the Nordic Seas than to *T. egelida* described from western Arctic and northern Greenland cores. No discernable difference seems to exist between the more abundant occurrences in MIS 5 and the earlier Pleistocene specimens from LOMROG12-7PC or AO16-5PC. As such, despite our initial excitement at finding *Turborotalita* spp. in two cores that share a coherent lithostratigraphy with the ACEX borehole, we do not think they represent the unique *T. egelida* zone that is a proposed biostratigraphic event marker in other parts of the Arctic (Cronin et al., 2014).

Paleoceanographic Implications

Nørgaard-Pedersen et al. (2007) argued that the large numbers of *T. quinqueloba* in GreenIce-11 suggests less severe perennial sea-ice conditions north of the Canada-Greenland margin during MIS 5. The coeval MIS 5 occurrences of *T. quinqueloba* in LOMROG12-7PC and AO16-5PC extend the geographical range over which this sub-polar planktic foraminifera is identified in the Arctic Ocean, indicating a much wider region of anomalous oceanographic conditions. A remarkable observation concerning these MIS 5 assemblages is that they tend to far exceed the abundance of *T. quinqueloba* found in Holocene core top sediments. In GreenIce-11, *T. quinqueloba* accounted for 20–35% of the >63 μm foraminifera assemblage in MIS 5.1 and 40–50% in MIS 5.5, but only 1% of the Holocene assemblage. This observation was supported by equally low numbers found in Holocene sediments from a series of box cores from the central Lomonosov Ridge and Eurasian Basin (**Figure 1**; Nørgaard-Pedersen et al., 2007). Our relative abundances are in line with these observations, and we note that no *T. quinqueloba* were found in the Holocene age core top sediments of LOMROG12-7PC or AO16-5PC.

The earlier Pleistocene appearances, currently dated between MIS 9 and 11 in LOMROG12-7PC and AO16-5PC, would also suggest more reduced sea-ice conditions, or similar anomalous paleoceanographic conditions in the Arctic, during earlier Pleistocene interglacials. Interglacials associated with MIS 5, 9, and 11 are all recognized as periods of pronounced warming in the Pleistocene (**Figure 10**; Past Interglacials Working Group of Pages, 2016). Further insights into the paleoceanographic conditions during Pleistocene interglacials require additional work to document absolute abundances and assemblage compositions in these new

records. These studies would benefit from the incorporation of additional cores from this region of the Lomonosov Ridge where better preservation of calcareous foraminifera are recorded, compared to the central region where *ACEX* was drilled.

The need for additional records comes from the sporadic occurrence of calcareous foraminifera both within and between sediment cores. For example, first order differences in relative foraminifera abundances are seen in stratigraphically coeval sections of LOMROG12-7PC and AO16-5PC, particularly between the D_B and the peach colored clay layer (PL) (**Figure 6**). This could reflect differences in productivity or could arise from variable rates of seafloor/post-depositional dissolution. Carbonate dissolution is often discussed in Arctic paleoceanography (Cronin et al., 2008) but has not yet been investigated in a level of detail comparable to regions like the Norwegian-Greenland Sea (Huber et al., 2000a). Many records from the central Arctic do appear to be severely affected by carbonate dissolution. This includes the *ACEX* record where over 1000 planktic foraminifera were found in each dry gram of sediment in MIS 1-3, but <1–2 individuals/g in selected intervals of older sediments (Eynaud et al., 2009; **Figure 10**).

Dissolution may be particularly problematic for the small thin-shelled specimens of *T. quinqueloba*. Volkmann (2000a) has suggested that low abundances of *T. quinqueloba* in surface sediments from the eastern Arctic, compared to their abundance in multi-net tows, may reflect this susceptibility to dissolution in the water column. Post-burial dissolution may also be a significant factor in their downcore occurrence where local changes in carbon export and burial at the seafloor may influence selective dissolution in some intervals. This may explain the apparent stratigraphic offset in the deeper occurrence of *T. quinqueloba* between LOMROG12-7PC and AO16-5PC. A broader and more detailed (quantitative) study of foraminifera abundances and assemblage composition from sediment cores on the Lomonosov Ridge off Greenland could help establish whether *T. quinqueloba* routinely entered the central Arctic during Pleistocene interglacials, or whether they were confined to specific MISs. The coherent lithostratigraphy found across this region of the Lomonosov Ridge (**Figure 5**) can facilitate these inter-site comparisons.

CONCLUSION

Three stratigraphic occurrences of the sub-polar planktic foraminifera genus *Turborotalita* are documented in two sediment cores from the Lomonosov Ridge. *Turborotalita* are not found in core top and Holocene samples from these cores. Based on the Pleistocene age model for *ACEX*, *Turborotalita* occurs in both cores during MIS 5.1 and 5.5, consistent with observations made on sediment cores located closer to the Greenland margin. An earlier Pleistocene occurrence does not appear to be stratigraphically coeval, occurring in MIS 9/10 in LOMROG12-7PC and MIS 11 in AO16-5PC.

Morphological observations on individual tests indicate a close affinity with *T. quinqueloba* from the Nordic Seas. The specimens differ from descriptions of *T. egelida* in the western Arctic, which is proposed as a marker for MIS 11 (Polyak et al., 2013; Cronin et al., 2014).

The occurrences of *T. quinqueloba* in LOMROG12-7PC and AO16-5PC further document the incursion of sub-polar planktic foraminifera into the central Arctic during some Pleistocene interglacials. We emphasize the importance of conducting *T. quinqueloba* analyses in both the >125 μm and <125 μm sediment fractions due to the often small size of this species in the central Arctic. Given its apparently narrow range of environmental and oceanic tolerances, this species has enormous potential for reconstructing regional Arctic Ocean climate during interglacials, including sea ice extent and northward penetration of warm water masses.

Future work is needed to (1) determine the taxonomic relationships between *T. quinqueloba* and *T. egelida*, (2) acquire additional age control to anchor the earlier appearances of *Turborotalita*, and (3) establish whether the intermittent occurrence in Pleistocene interglacials reflects anomalous oceanographic conditions or is a consequence of post-depositional dissolution.

AUTHOR CONTRIBUTIONS

MO, HC, and TC developed the concept for the article. MO, SK, and GW developed stratigraphic correlations between the sites, including preparation, and submission of samples for radiocarbon dating. HC contributed taxonomic analyses and SEM imaging. MJ, RG, LL, and SW were involved in the organization and implementation of the icebreaker led expeditions that recovered sediment cores presented in this manuscript, including generation of shipboard, and shore-based data. All authors contributed to the writing and editing of the text.

FUNDING

The Swedish Polar Research Secretariat, the Swedish Research Council (VR), and the Knut and Alice Wallenberg Foundation are thanked for supporting research cruises and laboratory facilities. TC was provided the funding by United States Geological Survey Land Change Program. MO was funded by the Swedish Research Council (DNR 2016-05092).

ACKNOWLEDGMENTS

We thank the captain and supporting crew of I/B *Oden* who made data collection on the multiple expeditions possible. Special thanks to Antastasia Zhuravleva, GEOMAR Helmholtz Centre for Ocean Research, Kiel, Germany, for loaning samples from cores M23063 and M23455 to aid with the comparative

taxonomy. We also thank Malvina Forbes and Anna Nyberg for their laboratory support at Stockholm University. Any use of trade, firm, or product names is for descriptive purposes only and does not imply endorsement by the United States Government. Data presented in this paper can be accessed via the Bert Bolin Centre for Climate Research database (https://bolin.su.se/data/oregan-2019).

SUPPLEMENTARY MATERIAL

The Supplementary Material for this article can be found online at: https://www.frontiersin.org/articles/10.3389/feart.2019.00071/full#supplementary-material

FIGURE S1 | Stratigraphic correlation of multiple records across ∼575 km of the Lomonosov Ridge. Here the K/Ti ratio from XRF-scanning data is illustrated using the correlations presented in **Figure 5** of the manuscript. The bold red correlative line indicates the position of a distinct fine-grained (95–100% clay) peach colored layer (labeled PL). Greek symbols (α, β, γ) highlight a correlative sequence of grain size and color variations that are recognised above the fine-grained peach colored layer (PL). The two diamicts found near the top of all the cores are labeled D_B and D_A.

FIGURE S2 | Stratigraphic correlation of multiple records across ∼575 km of the Lomonosov Ridge. Here the Mn/Ti ratio from XRF-scanning data is illustrated using the correlations presented in **Figure 5** of the manuscript. The bold red correlative line indicates the position of a distinct fine-grained (95–100% clay) peach colored layer (labeled PL). Greek symbols (α, β, γ) highlight a correlative sequence of grain size and color variations that are recognised above the fine-grained peach colored layer (PL). The two diamicts found near the top of all the cores are labeled D_B and D_A.

REFERENCES

Adler, R. E., Polyak, L., Crawford, K. A., Grottoli, A. G., Ortiz, J. D., Kaufman, D. S., et al. (2009). Sediment record from the western Arctic Ocean with an improved late quaternary age resolution: HOTRAX core HLY0503-8JPC, Mendeleev Ridge. *Glob. Planet. Chang* 68, 18–29. doi: 10.1016/j.gloplacha.2009.03.026

Alexanderson, H., Backman, J., Cronin, T. M., Funder, S., Ingólfsson, Ó, Jakobsson, M., et al. (2014). An arctic perspective on dating mid-late pleistocene environmental history. *Quat. Sci. Rev.* 92, 9–31. doi: 10.1016/j.quascirev.2013.09.023

Backman, J., Fornaciari, E., and Rio, D. (2009). Biochronology and paleoceanography of late pleistocene and holocene calcareous nannofossil abundances across the Arctic Basin. *Mar. Micropaleontol.* 72, 86–98. doi: 10.1016/j.marmicro.2009.04.001

Backman, J., Jakobsson, M., Frank, M., Sangiorgi, F., Brinkhuis, H., Stickley, C., et al. (2008). Age model and core-seismic integration for the Cenozoic ACEX sediments from the lomonosov ridge. *Paleoceanography* 23, 1–15. doi: 10.1029/2007PA001476

Backman, J., Jakobsson, M., Løvlie, R., Polyak, L., and Febo, L. A. (2004). Is the central arctic ocean a sediment starved basin? *Quat. Sci. Rev.* 23, 1435–1454. doi: 10.1029/2007PA001476

Bauch, H. A. (1997). "Paleoceanography of the North Atlantic Ocean (68°–76°N) during the past 450 ky deduced from planktic foraminiferal assemblages and stable isotopes," in *Contributions to the Micropaleontology and Paleoceanography of the Northern North Atlantic*, eds H. C. Hass and M. A. Kaminski (Krakow: Grzybowski Foundation Special Publication), 83–100. doi: 10.1016/j.quascirev.2003.12.005

Carstens, J., and Wefer, G. (1992). Recent distribution of planktic foraminifera in the Nansen Basin, Arctic Ocean. *Deep Sea Res. Part I* 39, 507–524. doi: 10.1016/S0198-0149(06)80018-X

Chawchai, S., Kylander, M. E., Chabangborn, A., L€owemark, L., and Wohlfarth, B. (2016). Testing commonly used X-ray fluorescence core scanning-based proxies for organic-rich lake sediments and peat. *Boreas* 45, 180–189. doi: 10.1111/bor.12145

Cifelli, R., and Smith, R. K. (1970). Distribution of planktic foraminifera in the vicinity of the North Atlantic Current. *Smithson. Contrib. Paleobiol.* 4, 359–866.

Clark, D. L. (1970). Magnetic reversals and sedimentation rates in the Arctic Ocean. *Geol. Soc. Am. Bull.* 81, 3129–3134. doi: 10.1130/0016-7606(1970)81[3129:MRASRI]2.0.CO;2

Clark, D. L., Whitman, R. R., Morgan, K. A., and Mackey, S. D. (1980). Stratigraphy and glacial-marine sediments of the amerasian basin, central arctic ocean. *Geol. Soc. Am.* 181, 1–57. doi: 10.1130/SPE181-p1

Cronin, T., Eynaud, F., Smith, S., O'Regan, M., and King, J. (2008). Quaternary paleoceanography of the central Arctic based on IODP ACEX 302 foraminiferal assemblages. *Paleoceanography* 23:PA1S18. doi: 10.1029/2007PA001484

Cronin, T. M., DeNinno, L. H., Polyak, L., Caverly, E. K., Poore, R. Z., Brenner, A., et al. (2014). Quaternary ostracode and foraminiferal biostratigraphy and paleoceanography in the western Arctic Ocean. *Mar. Micropaleontol.* 111, 118–133. doi: 10.1016/j.marmicro.2014.05.001

Cronin, T. M., Polyak, L., Reed, D., Kandiano, E. S., Marzen, R. E., and Council, E. A. (2013). A 600-ka arctic sea-ice record from mendeleev ridge based on ostracodes. *Quat. Sci. Rev.* 79, 157–167. doi: 10.1016/j.quascirev.2012.12.010

Darling, F. K., and Wade, M. C. (2008). The genetic diversity of planktic foraminifera and the global distribution of ribosomal RNA genotypes. *Mar. Micropaleontol.* 67, 216–238. doi: 10.1016/j.marmicro.2008.01.009

Darling, K. F., Kucera, M., and Wade, C. M. (2007). Global molecular phylogeography reveals persistent arctic circumpolar isolation in a marine planktonic protest. *Proc. Natl. Acad. Sci. U.S.A.* 104, 5002–5007. doi: 10.1073/pnas.0700520104

En ISO 14688-1:2018 (2018). *Geotechnical Investigation and Testing – Identification and Classification of Soil – Part 1: Identification and Description*. Brussels: Comité Européen de Normalisation.

Eynaud, F. (2011). Planktonic foraminifera in the Arctic: potentials and issues regarding modern and quaternary populations. *IOP Conf. Ser. Earth Environ. Sci.* 14:012005. doi: 10.1088/1755-1315/14/1/012005

Eynaud, F., Cronin, T. M., Smith, S. A., Zaragosi, S., Mavel, J., Mary, Y., et al. (2009). Morphological variability of the planktic foraminifer neogloboquadrina pachyderma from ACEX cores: implications for late pleistocene circulation in the Arctic Ocean. *Micropaleontology* 55, 101–116.

Frank, M., Backman, J., Jakobsson, M., Moran, K., O'Regan, M., King, J., et al. (2008). Beryllium isotopes in central Arctic Ocean sediments over the past 12.4 million years: stratigraphic and paleoceanographic implications. *Paleoceanography* 23:PA1S02. doi: 10.1029/2007PA001478

Hanslik, D. (2011). *Late Quaternary Biostratigraphy and Paleoceanography of the Central Arctic Ocean*. Stockholm: Department of Geological Sciences Stockholm University, 32.

Hanslik, D., Jakobsson, M., Backman, J., Björck, S., Sellén, E., O'Regan, M., et al. (2010). Quaternary Arctic Ocean sea ice variations and radiocarbon reservoir age corrections. *Quat. Sci. Rev.* 29, 3430–3441. doi: 10.1016/j.quascirev.2010.06.011

Hanslik, D., Löwemark, L., and Jakobsson, M. (2013). Biogenic and detrital-rich intervals in central Arctic Ocean cores identified using x-ray fluorescence scanning. *Polar Res.* 32:18386. doi: 10.3402/polar.v32i0.18386

Herman, Y. (1974). "Arctic Ocean sediments, microfauna, and the climatic record in late Cenozoic time," in *Marine Geology and Oceanography of the Arctic Seas*, ed. Y. Herman (Berlin: Springer), 283–348.

Hillaire-Marcel, C., Ghaleb, B., de Vernal, A., Maccali, J., Cuny, K., Jacobel, A., et al. (2017). A new chronology of late quaternary sequences from the central Arctic Ocean based on "extinction ages" of their excesses in 231Pa and 230Th. *Geochem. Geophys. Geosyst.* 18, 4573–4585. doi: 10.1002/2017GC007050

Huber, R., Meggers, H., Baumann, K.-M., Raymo, M. E., and Henrich, R. (2000a). Recent and pleistocene carbonate dissolution in sediments of the Norwegian–Greenland Sea. *Mar. Geol.* 165, 123–136. doi: 10.1016/S0025-3227(99)00138-3

Huber, R., Meggers, H., Baumann, K.-M., Raymo, M. E., and Henrich, R. (2000b). Shell size variation of the planktonic foraminifer neogloboquadrina pachyderma sin. in the norwegian-greenland sea during the last 1.3 Myrs: implications for paleoceanographic reconstructions. *Palaeogeogr. Palaeoclimatol. Palaeoecol.* 160, 193–212. doi: 10.1016/S0031-0182(00)00066-3

Husum, K., and Hald, M. (2012). Arctic planktic foraminiferal assemblages: implications for subsurface temperature reconstructions. *Mar. Micropaleontol.* 96-97, 38–47. doi: 10.1016/j.marmicro.2012.07.001

Jakobsson, M., Backman, J., Murray, A., and Løvlie, R. (2003). Optically stimulated luminescence dating supports central arctic ocean cm-scale sedimentation rates. *Geochem. Geophys. Geosyst.* 4:1016. doi: 10.1029/2002GC000423

Jakobsson, M., Løvlie, R., Al-Hanbali, H., Arnold, E., Backman, J., and Mörth, M. (2000). Manganese and color cycles in Arctic Ocean sediments constrain pleistocene chronology. *Geology* 28, 23–26. doi: 10.1130/0091-7613(2000)28<23:MACCIA>2.0.CO;2

Jakobsson, M., Løvlie, R., Arnold, E. M., Backman, J., Polyak, L., Knutsen, J. O., et al. (2001). Pleistocene stratigraphy and paleoenvironmental variation from lomonosov ridge sediments, central Arctic Ocean. *Glob. Planet. Chang* 31, 1–22. doi: 10.1016/S0921-8181(01)00110-2

Johannessen, T., Jansen, E., Flatøy, A., and Ravelo, A. C. (1994). "The relationship between surface water masses, oceanographic fronts and paleoclimatic proxies in surface sediments of the Greenland, Iceland, Norwegian Seas," in *Carbon Cycling in Glacial Ocean: Constraints on the Ocean's Role in Global Change*, eds R. Zahn, M. Kominski, and L. Labyrie (New York, NY: Springer-Verlag), 61–85.

Kandiano, E. S., and Bauch, H. A. (2002). A case study on the application of different planktic foraminiferal size fractions for interpreting late quaternary paleoceanographic changes in the polar North Atlantic. *J. Foraminifer. Res.* 32, 245–251. doi: 10.2113/32.3.245

Kandiano, E. S., Bauch, H. A., Fahl, K., Helmke, J. O., Röhl, U., Perez-Folgado, M., et al. (2012). The meridional temperature gradient in the eastern North Atlantic during MIS 11 and its link to the ocean–atmosphere system. *Palaeogeogr. Palaeoclimatol. Palaeoecol.* 333-334, 24–29. doi: 10.1016/j.palaeo.2012.03.005

Kimoto, K., and Tsuchiya, M. (2006). The "unusual" reproduction of planktic foraminifera:: an asexual reproductive phase of neogloboquadrina pachyderma (Ehrenberg). *Anuário do Instituto de Geociências-UFRJ* 29:461.

Kucera, M., Weinelt, M., Kiefer, T., Pflaumann, U., Hayes, A., Weinelt, M., et al. (2005a). Compilation of planktic foraminifera census data, modern from the Atlantic Ocean. *PANGAEA*. doi: 10.1594/PANGAEA.227322 (accessed July 1, 2018).

Kucera, M., Weinelt, M., Kiefer, T., Pflaumann, U., Hayes, A., Weinelt, M., et al. (2005b). Reconstruction of sea-surface temperatures from assemblages of planktic foraminifera: multi-technique approach based on geographically constrained calibration data sets and its application to glacial Atlantic and Pacific Oceans. *Quat. Sci. Rev.* 24, 951–998. doi: 10.1016/j.quascirev.2004.07.014

Lisiecki, L., and Raymo, M. (2005). A pliocene-pleistocene stack of 57 globally distributed benthic δ18O records. *Paleoceanography* 20:PA1003.

Löwemark, L., Chao, W.-S., Gyllencreutz, R., Hanebuth, T. J. J., Chiu, P.-Y., Yang, T.-N., et al. (2016). Variations in glacial and interglacial marine conditions over the last two glacial cycles off northern Greenland. *Quat. Sci. Rev.* 147, 164–177. doi: 10.1016/j.quascirev.2015.10.035

Löwemark, L., März, C., O'Regan, M., and Gyllencreutz, R. (2014). Arctic ocean Mn-stratigraphy: genesis, synthesis and inter-basin correlation. *Quat. Sci. Rev.* 92, 97–111. doi: 10.1016/j.quascirev.2013.11.018

Löwemark, L., O'Regan, M., Hanebuth, T. J. J., and Jakobsson, M. (2012). Late quaternary spatial and temporal variability in Arctic deep-sea bioturbation and its relation to Mn cycles. *Palaeogeogr. Palaeoclimatol. Palaeoecol.* 365–366, 192–208. doi: 10.1016/j.palaeo.2012.09.028

Lüthi, D., Le Floch, M., Bereiter, B., Blunier, T., Barnola, J.-M., Siegenthaler, U., et al. (2008). High-resolution carbon dioxide concentration record 650,000 - 800,000 years before present. *Nature* 453, 379–382. doi: 10.1038/nature06949

Marzen, R. E., DeNinno, L. H., and Cronin, T. M. (2016). Calcareaous microfossil-based orbital cyclostratigraphy in the Arctic. *Quat. Sci. Rev.* 149, 109–121. doi: 10.1016/j.quascirev.2016.07.004

Nørgaard-Pedersen, N., Mikkelsen, N., Lassen, S. J., Kristoffersen, Y., and Sheldon, E. (2007). Reduced sea ice concentrations in the Arctic Ocean during the last interglacial period revealed by sediment cores off northern Greenland. *Paleoceanography* 22, 1–15. doi: 10.1029/2006PA001283

Nørgaard-Pedersen, N., Spielhagen, R. F., Thiede, J., and Kassens, H. (1998). Central Arctic surface ocean environment during the past 80,000 years. *Paleoceanography* 13, 193–204. doi: 10.1029/97PA03409

Olsson, R. K., and Hemleben, C. (2006). "Wall textures of Eocene planktonic foraminifera," in *Atlas of Eocene planktonic foraminifera, Cushman Foundation of Foraminiferal Research, Special Publication no. 41: Lawrence*, eds P. N. Pearson, R. K. Olsson, C. Hemleben, B. T. Huber, and W. A. Berggren (Kansas: Allen Press), 47–66.

O'Regan, M. (2011). Late Cenozoic paleoceanography of the central Arctic Ocean. *IOP Conf. Ser. Earth Environ. Sci.* 14:012002. doi: 10.1088/1755-1315/14/1/012002

O'Regan, M., King, J., Backman, J., Jakobsson, M., Pälike, H., Moran, K., et al. (2008a). Constraints on the Pleistocene chronology of sediments from the lomonosov ridge. *Paleoceanography* 23:PA1S19. doi: 10.1029/2007PA001551

O'Regan, M., Sakamoto, T., and King, J. (2008b). "Data Report: Regional stratigraphic correlation and a revised composite depth scale for IODP Expedition 302," in *Proc IODP Sci. Results, 302*, eds J. Backman, K. Moran, D. B. McInroy, and L. A. Mayer (Edinburgh: Integrated Ocean Drilling Program Management International, Inc), doi: 10.2204/iodp.proc.302.202.2008

O'Regan, M., Sellén, E., and Jakobsson, M. (2014). Middle to late quaternary grain size variations and sea-ice rafting on the lomonosov ridge. *Polar Res.* 33:23672. doi: 10.3402/polar.v33.23672

O'Regan, M., St. John, K., Moran, K., Backman, K., King, J., Haley, B. A., et al. (2010). Plio-Pleistocene trends in ice rafted debris on the lomonosov ridge. *Quat. Int.* 219, 168–176. doi: 10.1016/j.quaint.2009.08.010

Pados, T., and Spielhagen, R. F. (2014). Species distribution and depth habitat of recent planktic foraminifera in Fram Strait, Arctic Ocean. *Polar Res.* 33:22483. doi: 10.3402/polar.v33.22483

Past Interglacials Working Group of Pages (2016). Interglacials of the last 800,000 years. *Rev. Geophys.* 54, 162–219. doi: 10.1002/2015RG000482

Phillips, R. L., and Grantz, A. (2001). Regional variations in provenance and abundance of icerafted clasts in arctic ocean sediments: implications for the configuration of late quaternary oceanic and atmospheric circulation in the arctic. *Mar. Geol.* 172, 91–115. doi: 10.1016/S0025-3227(00)00101-8

Polyak, L., Best, K. M., Crawford, K. A., Council, E. A., and St-Onge, G. (2013). Quaternary history of sea ice in the western Arctic Ocean based on foraminifera. *Quat. Sci. Rev.* 79, 145–156. doi: 10.1016/j.quascirev.2012.12.018

Poore, R. Z., Ishman, S. E., Phillips, R. L., and McNeil, D. H. (1994). Quaternary stratigraphy and paleoceanography of the Canada Basin, Western Arctic Ocean. *U.S. Geol. Surv. Bull.* 280:32. doi: 10.3133/b2080

Poore, R. Z., Phillips, R. L., and Rieck, H. J. (1993). Paleoclimate record for northwind ridge, western Arctic Ocean. *Paleoceanography* 8, 149–159. doi: 10.1029/93PA00146

Reimer, P. J., Bard, E., Bayliss, A., Beck, J. W., Blackwell, P. G., Bronk, R. C., et al. (2013). IntCal13 and Marine13 radiocarbon age calibration curves 0-50,000 years cal BP. *Radiocarbon* 55, 1869–1887. doi: 10.1016/j.dib.2018.10.040

Risebrobakken, B., and Berben, S. M. P. (2018). Early holocene establishment of the barents sea Arctic Front. *Front. Earth Sci.* 6:166. doi: 10.3389/feart.2018.00166

Rothwell, R. G., and Croudace, I. W. (2015). Twenty years of XRF core scanning marine sediments: what do geochemical proxies tell us? in Croudace, I. W., Rothwell, R. G. (eds.) *Micro-XRF Studies of Sediment Cores: Applications of a Non-destructive tool for the Environmental Sciences* (Dordrecht: Springer) 688. doi: 10.1007/978-94-017-9849-5_2

Schiebel, R., and Hemleben, C. (2017). *Planktic Foraminifera in the Modern Ocean*. Heidelberg: Springer-Verlag, 161. doi: 10.1007/978-3-662-50297-6

Schiebel, R., Spielhagen, R. F., Garnier, J., Hagemann, J., Howa, H., Jentzen, A., et al. (2017). Modern planktic foraminifers in the high-latitude ocean. *Mar. Micropaleontol.* 136, 1–13. doi: 10.1016/j.marmicro.2017.08.004

Schlitzer, R. (2018). *Ocean Data View*. Available at: http://odv.awi.de (accessed July 1, 2018).

Schreck, M., Nam, S.-I., Polyak, L., Vogt, C., Kong, G. S., Stein, R., et al. (2018). Improved pleistocene sediment stratigraphy and paleoenvironmental implications for the western Arctic Ocean off the East Siberian and Chukchi margins. *Arktos* 4:21. doi: 10.1007/s41063-018-0057-8

Sellén, E., O'Regan, M., and Jakobsson, M. (2010). Spatial and temporal arctic ocean depositional regimes: a key to the evolution of ice drift and current patterns. *Quat. Sci. Rev.* 29, 3644–3664. doi: 10.1016/j.quascirev.2010.06.005

Spielhagen, R. F., Baumann, K.-H., Erlenkeuser, H., Nowaczyk, N. R., Nørgaard-Pedersen, N., Vogt, C., et al. (2004). Arctic Ocean deep-sea record of northern Eurasian ice sheet history. *Quat. Sci. Rev.* 23, 1455–1483.

Stein, R. (2008). *Arctic Ocean Sediments: Processes, Proxies, and Paleoenvironment*, Vol. 2. Bremerhaven: Elsevier Science.

Stein, R., Matthiessen, J., Niessen, F., Bazhenova, E., Krylov, A., and Nam, S. (2010). Towards a better (litho-) stratigraphy and reconstruction of quaternary

paleoenvironment in the Amerasian basin (Arctic Ocean). *Polarforschung* 79, 97–121.

Stuiver, M., Reimer, P. J., and Reimer, R. W., (2018). *CALIB 7.1 [WWW Program]*. Available at: http://calib.org (accessed June 18, 2018).

Thierstein, H. R., Geitzenauer, K. R., Molino, B., and Shackleton, N. J. (1977). Global synchroneity of late Quaternary coccolith datum levels: validation by oxygen isotopes. *Geology* 5, 400–404. doi: 10.1130/0091-7613(1977)5<400:GSOLQC>2.0.CO;2

Van Nieuwenhove, N., Bauch, H. A., Eynaud, F., Kandiano, E., Cortijo, E., and Turon, J.-L. (2011). Evidence for delayed poleward expansion of North Atlantic surface waters during the last interglacial (MIS 5e). *Quat. Sci. Rev.* 30, 934–946. doi: 10.1016/j.quascirev.2011.01.013

Volkmann, R. (2000a). *Planktic Foraminifer Ecology and Stable Isotope Geochemistry in the Arctic Ocean: Implications from Water Column and Sediment Surface Studies for Quantitative Reconstructions of Oceanic Parameters*. Bremerhaven: Alfred Wegener Institute for Polar and Marine Research.

Volkmann, R. (2000b). Planktic foraminifers in the outer laptev sea and the fram strait - modern distribution and ecology. *J. Foraminifer. Res.* 3, 157–176. doi: 10.2113/0300157

Xuan, C., and Channell, J. E. T. (2010). Origin of apparent magnetic excursions in deep-sea sediments from mendeleev-alpha ridge, arctic ocean. *Geochem. Geophys. Geosyst.* 11:Q02003. doi: 10.1029/2009GC002879

Xuan, C., Channell, J. E. T., Polyak, L., and Darby, D. A. (2012). Paleomagnetism of quaternary sediments from lomonosov ridge and yermak plateau: implications for age models in the Arctic Ocean. *Quat. Sci. Rev.* 32, 48–63. doi: 10.1016/j.quascirev.2011.11.015

Conflict of Interest Statement: The authors declare that the research was conducted in the absence of any commercial or financial relationships that could be construed as a potential conflict of interest.